JOURNAL OF GEOPHYSICAL RESEARCH, VOL. 105, NO. D14, PAGES 17,911–17,924, JULY 27, 2000

A continental outbreak of air during the Second Aerosol Characterization Experiment (ACE 2): A Lagrangian experiment

Karsten Suhre, [1] Doug W. Johnson, [2] Céline Mari, [1] Robert Rosset, [1] Simon Osborne, [2] Robert Wood, [2] Timothy S. Bates, [3] and Frank Raes [4]

Abstract. A mesoscale meteorological model is used to simulate the continental outbreak of air that occured over North Atlantic Ocean during the Second Aerosol Characterization Experiment (ACE 2). Comparison with Meteosat 6 visible images shows that the model is able to reproduce most of the observed cloud features in the entire modeling domain, including a frontal system, orographic clouds over the Pyrenees and the Iberian Peninsula, boundary layer clouds in the ACE 2 region, and cloud-free areas in the dry air outflow off the Portuguese coast. The model reproduces correctly the temperature, humidity, wind speed and direction, cloud water content, and light precipitation events observed by the aircraft during the Lagrangian experiment, while following a tagged boundary layer air parcel over a 28-hour long period. A passive tracer, introduced in the model at the time corresponding to the balloon launch, followed the balloon track with an error in position that is smaller than 1° after 24-hours with about 20% higher speed. An estimate of the boundary layer entrainment velocity is obtained, based on observed boundary layer growth rates and modeled vertical wind speed. The average entrainment velocity of 1.28 cm/s for the 28-hour Lagrangian period agrees with experimentally derived entrainment velocities.

1. Introduction

One goal of the International Global Atmospheric Chemistry (IGAC) project's Aerosol Characterization Experiments (ACE) is to reduce the uncertainty in the calculation of climate forcing by aerosols by improving the aerosol representation in regional and global scale models [*Bates et al.*, 1998]. We present here an evaluation of a regional model in terms of its capacity to simulate boundary layer dynamics and cloud formation at the mesoscale.

A first experiment (ACE 1) was conducted in November/December 1995 under clean maritime conditions over the Southern Ocean [*Bates et al.*, 1998]. The present model was applied to investigate of dimethyl sulfide (DMS) oxidation and transport in the unpolluted marine boundary layer [*Mari et al.*, 1998]. The second ACE experiment (ACE 2) focused on anthropogenic aerosols from the European continent as they move out over the North Atlantic Ocean. The experiment took place in June-July 1997 between the Portuguese coast and the Canary islands. This area was affected by European outbreaks of polluted air that occur frequently during the summer months [*Raes et al.*, 2000]. A third ACE experiment (ACE Asia) is planned to start in 2001 in the heavily polluted air east of the Asian continent (B. Huebert et al., ACE Asia Survey and Evolution Component (AASEC) NSF Large Field Program scientific overview, 1999, available at http://saga.pmel.noaa.gov/aceasia/si_nsf).

Central to the ACE experiments, and in particular to the observation of the time evolution of aerosol properties, is the concept of Lagrangian experiments [*Huebert et al.*, 1996]. In such experiments a marine boundary layer air parcel is tagged using one or several constant-altitude balloons [*Businger et al.*, 1996, 1999]. These are then followed for 1-2 days by one or several research aircraft. Two such experiments were successful in ACE 1 [*Bates et al.*, 1998] and three were successfluin ACE 2 [*Johnson et al.*, 2000]. In an ideal setting, this approach eliminates the advective contribution from the budget equation of any observed variable, such as the concentration of aerosol number and mass or that of a reactive chemical species in the atmospheric boundary layer. The remaining unknowns to be determined are the deposition or emission fluxes at the surface and the entrainment fluxes across the boundary layer top. In reality, however, the marine boundary layer (MBL) rarely behaves like an idealized well mixed box, but rather like a one-dimensional vertically differentiated column [*Suhre and Rosset*, 1994; *Bretherton and Pincus*, 1995; *Russel et al.*, 1998; *Suhre et al.*, 1998; *Mari et al.*, 1999; *Wang et al.*, 1999]. This compli-

[1] Laboratoire d'Aérologie, UMR CNRS/Université Paul Sabatier, Toulouse, France.

[2] Meteorological Research Flight, Meteorological Office, Farnborough, England, UK.

[3] Pacific Marine Environmental Laboratory, NOAA, Seattle, Washington.

[4] Joint Research Centre, Ispra, Italy.

Paper number 2000JD900157.
0148-0227/00/2000JD900157$09.00

cates considerably the application of zero-dimensional box models in aerosol budget studies.

Here, we focus our analysis on the mesoscale meteorological modeling of the second Lagrangian experiment of ACE 2 [*Osborne et al.*, 2000]. The model may help shed light on the history of the air parcel prior to the launch of the balloons and on the origin of the observed vertical structure of the Lagrangian air column. It also allows the derivation of boundary layer entrainment velocities for use in Lagrangian box models. The evaluation from a meteorological point of view of such an Eulerian simulation compared to Lagrangian observations is essential for model improvement: this type of regional model will be used in the assessment of the aerosol radiative forcing over the Atlantic Ocean.

We will thus address the following questions:

1. How well can an Eulerian mesoscale model simulate the meteorological parameters that are essential for the aerosol radiative forcing over the Atlantic Ocean? In particular, what is the time evolution of the boundary layer vertical structure, large-scale subsidence, and formation of clouds?

2. What is the history of the air mass prior to the Lagrangian experiment? In particular, what is the origin of the pollution layer topping the MBL at the beginning of the experiment? When did cloud formation start? Were there previous cloud events that might have shaped the observed aerosol size spectrum in the MBL?

3. How does the entrainment velocity at the top of the boundary layer evolve in time? What is its average value?

2. Model Description

The model used in this study is the nonhydrostatic mesoscale meteorological model, Méso-NH, of Laboratoire d'Aérologie and Météo France [*Lafore et al.*, 1998]. Subgrid-scale turbulent mixing is described using a 1.5 order closure approach and a nonlocal mixing length scheme [*Redelsperger and Sommeria*, 1981; *Bougeault and Lacarrère*, 1989]. Deep convection parameterization is based on the flux conservative approach of *Kain and Fritsch* [1990], recently improved (P. Bechtold et al., A mass flux convection scheme for regional and global models, submitted to *Quartely Journal of the Royal Meteorological Society*, 2000). The classical *Kessler* [1969] bulk warm cloud microphysical scheme is used to model three water variables: vapor, cloud, and rain. A partial cloudiness scheme [*Bechtold et al.*, 1992] represents fractional cloud cover in grid cells near saturation. Visible and infrared radiative heating and cooling, in particular of the ground and in clouds, is calculated using the European Centre for Medium-Range Weather Forecasts (ECMWF) scheme [*Morcrette*, 1989]. This scheme is essential for the generation of turbulence induced by cloud top radiative cooling. Surface heat and momentum fluxes are derived using a prognostic surface scheme with two reservoirs in the ground. The sea surface temperature evolves from the ECMWF analyses. The model is set up with a horizontal resolution of 40 km on a 80 by 80 grid with 72 vertical levels (see Figure 1 for the model domain). To represent the relatively thin stratocumulus clouds that prevail in the ACE-2 region, it is essential to work with a high vertical resolution. A grid spacing of 40 m between the ground and an altitude of 1200 m, then increasing gradually by 7% per model level is applied. The model top at 14 km is in the stratosphere. A damping layer is active above 10 km to absorb gravity waves that may be reflected from the top of the model. Initial and boundary conditions are taken from ECMWF and are interpolated linearly between every 6 hourly analysis.

The simulation is started on July 15, 1997 at 1200 UTC, 36 hours prior to the start of the Lagrangian experiment. The total integration time is 72 hours using a 40 s timestep. For later analysis, model results are stored every 3 hours.

To compare the mesoscale simulation in a Lagrangian manner with the aircraft observations, a passive tracer is initialized in the model at the launch point of the balloon [*Mari et al.*, 1998]. This tracer is transported by the model using the same advection, turbulence, and convection algorithms as for the water variables. Following the center of mass of this tracer, vertical profiles of all model variables are extracted every 10 min. Prior to balloon launch, profiles are extracted from the 3-hourly model fields following the numerical, constant altitude backward trajectory presented in Figure 2. This trajectory was generated using the HYSPLIT_4 trajectory model [*Draxler and Hess*, 1998]. Excellent agreement between the numerical forward trajectory and the observed balloon trajectory (Figure 2) gives us confidence in the quality of the backward trajectory.

3. Dynamics and Aerosols Observed During the Lagrangian Experiment

In this study, we will concentrate on the second Lagrangian experiment of ACE 2 [*Osborne et al.*, 2000]. As outlined by *Johnson et al.* [2000], this is the ACE 2 Lagrangian experiment that is the most interesting with respect to cloud processing of aerosols. During the Lagrangian 2 experiment the seawater temperature under the Lagrangian air column increased by 1.8° while the mean wind speed near the surface decreased from 11.5 to 8.5 m/s. Decoupling of the marine boundary layer (MBL) occurred through the daytime hours of July 17, with weak decoupling still present at night toward the end of the experiment. The depth of the MBL doubled within the first 10 hours of the experiment. A pollution layer, rich in aerosol number, ozone, and carbon monoxide and extending up to 1800 m altitude topped a 500 m thick MBL at the moment of the balloon release. Entrainment of this elevated pollution layer into the MBL due to boundary layer growth and large-scale subsidence makes it an important contribution to the budget equations of the different aerosol and chemical variables. SO_2 concentrations decreased from 800 ppt to 200 ppt over the first 12 hours and formation of a bimodal aerosol spectrum during the first 10 hours was observed. Cloud processing considerably modified the aerosol spectrum in the size range 0.1-0.5 μm. *Dore et al.* [2000] show that this can be explained by production of sulphate in cloud droplets. Drizzle was only reaching surface during first flight, and even then sporadically and at a low rate. Modification of the cloud condensation nuclei (CCN) spec-

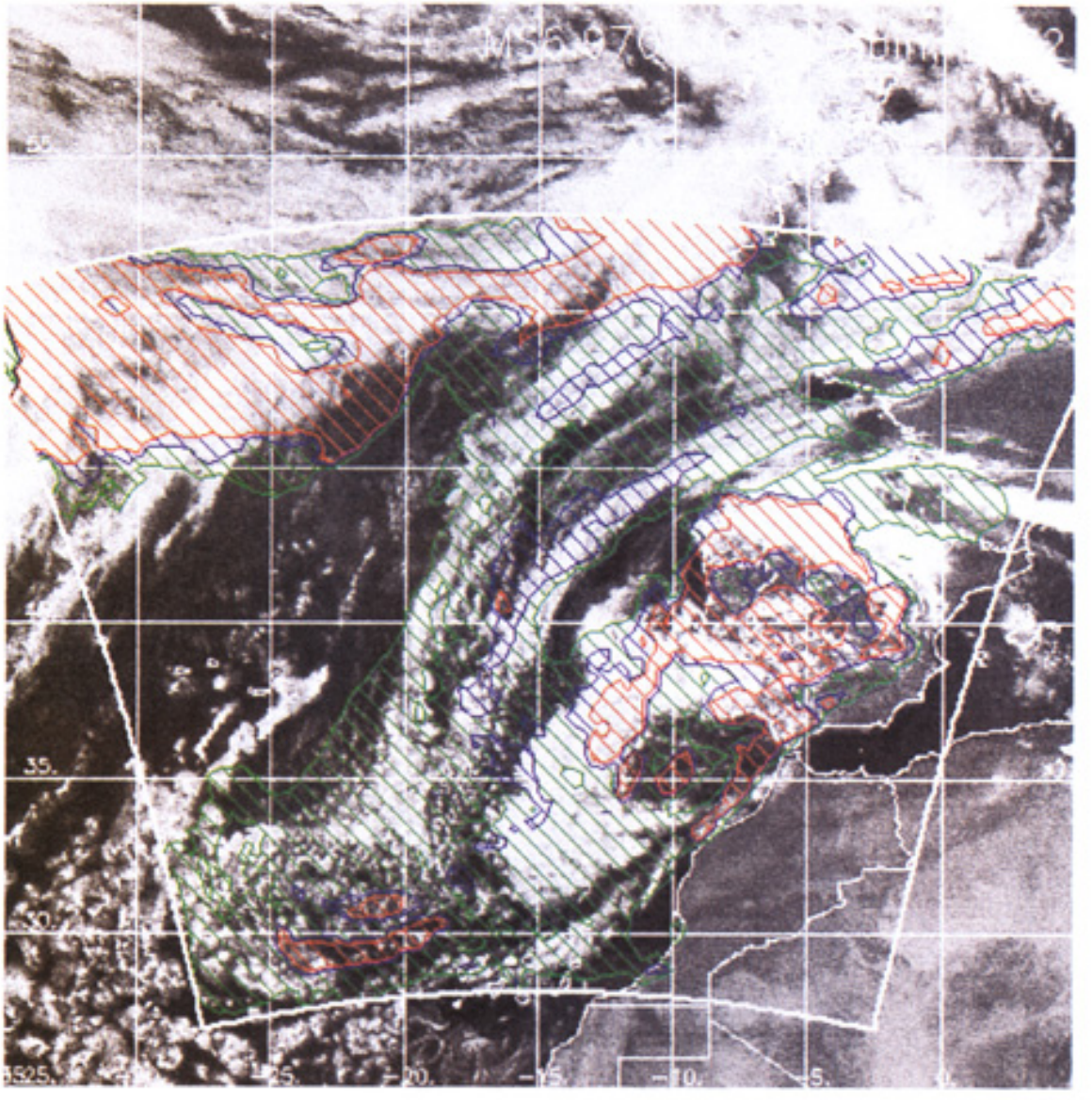

Plate 1. Meteosat 6 visible image of July, 16 1997 at 1200 UTC. The mesoscale model domain is represented by the truncated cone. Regions with one to four vertical levels with nonzero liquid water content are indicated by the green hatched regions. Regions with five to eight cloudy levels are indicated in blue and those with more than eigth levels are shown in red.

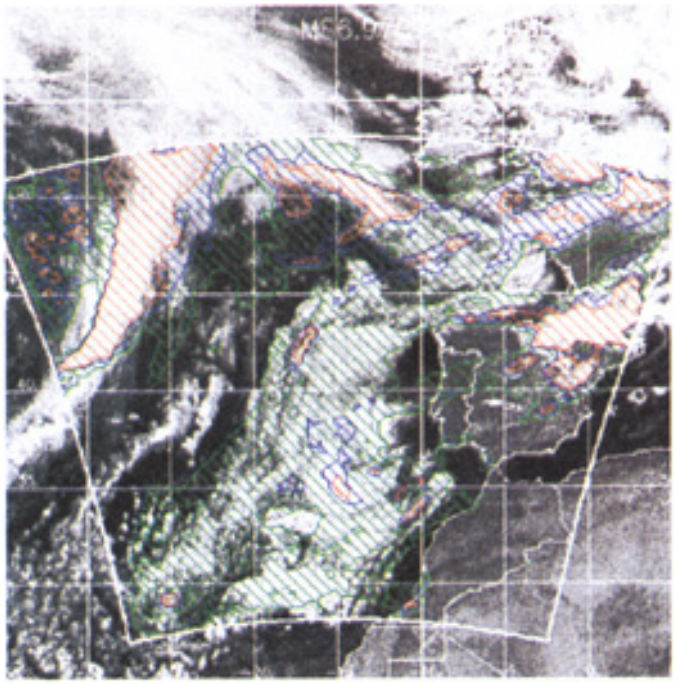

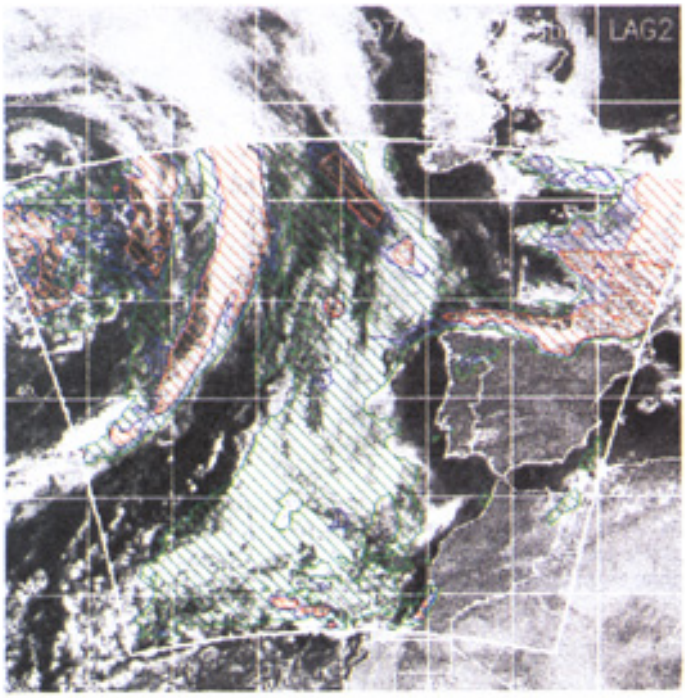

Plate 2. (Top) Same as Plate 1, but for July 17, 1997 at 1200 UTC,
Plate 3. (Bottom) Same as Plate 1, but for July 18, 1997 at 1200 UTC.

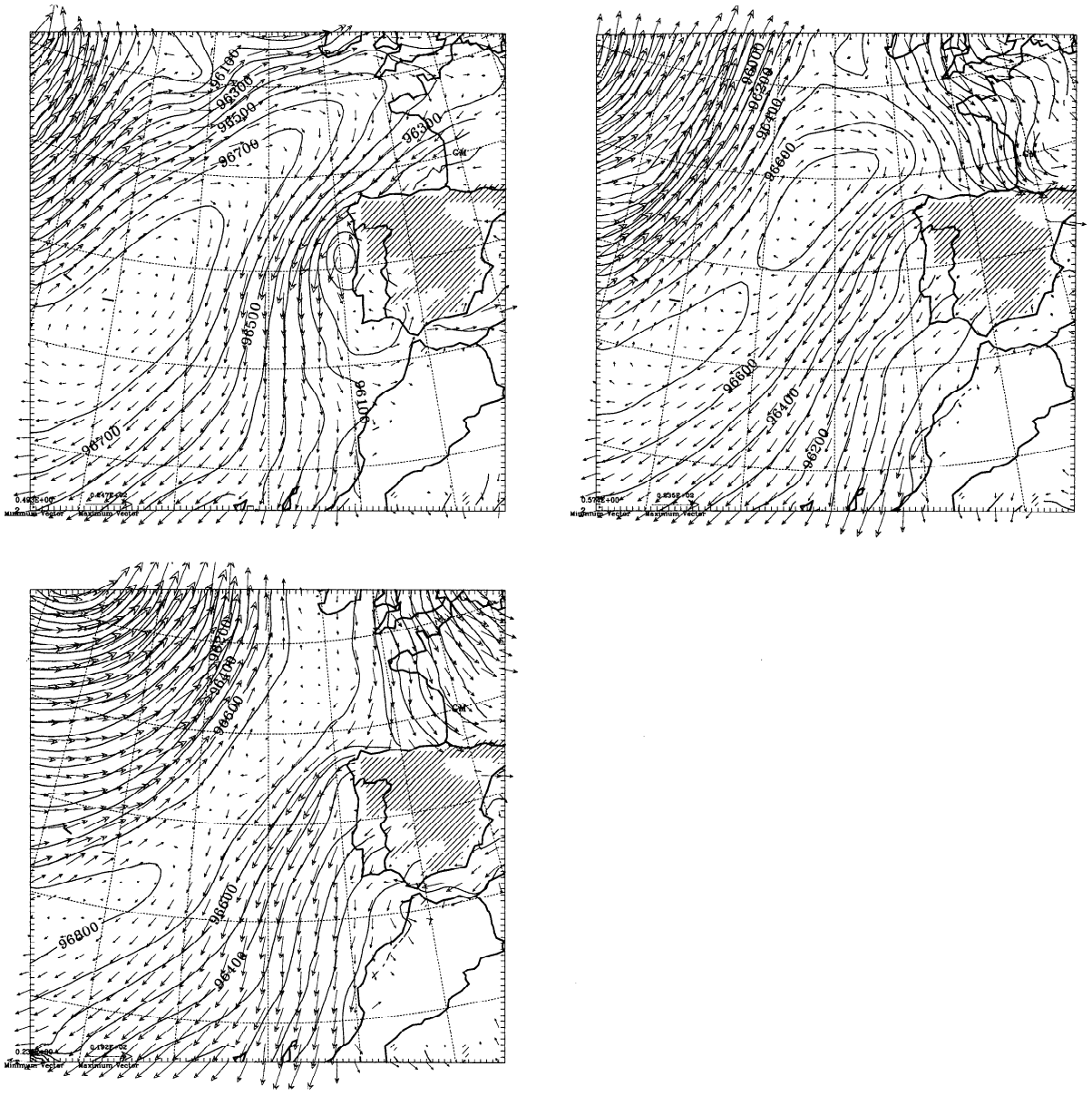

Figure 1. Wind vectors and atmospheric pressure at 500 m as simulated by Méso-NH at 1200 UTC on July 16, 17, and 18, 1997 (from left to right, and top to bottom).

trum thus occurred through cloud processing. This, together with changes in the dynamics of the marine boundary layer, affects the cloud physics and hence may have implications for the indirect radiative forcing by the aerosols.

4. Model Results

4.1. Comparison With Satellite Images

A comparison with Meteosat 6 visible images is performed to evaluate the capability of the model to reproduce the observed cloud fields. The general mesoscale flow pattern in the ACE 2 region is shown in Figure 1 and the associated cloud fields as seen by the Meteosat 6 visible imagery are presented in Plates 1-3. The modeled cloud fields after 24, 48, and 72 hours of simulation are plotted over the Meteosat image for direct intercomparison. It can be seen that the general features of cloudy/noncloudy parts in this anti-cyclonic situation are well reproduced, even in the inflow regions near the model boundaries. This demonstrates the high quality of the ECMWF analyses that are giving the lateral forcing conditions. Low-level maritime clouds, which are most effective in terms of indirect aerosol radiative forcing, are well depicted by the simulation. The transition of a dry, continental air mass flowing off the Iberian Peninsula to a cloudy, maritime air mass after humidification over the ocean can be seen in the satellite images of July 17 and 18. This transition is also captured by the model. It is in such an air mass that the Lagrangian balloons were launched. There are of course some minor shortcomings to this simulation. In particular, a cloud located between 35° and 42°N and around 25°W on

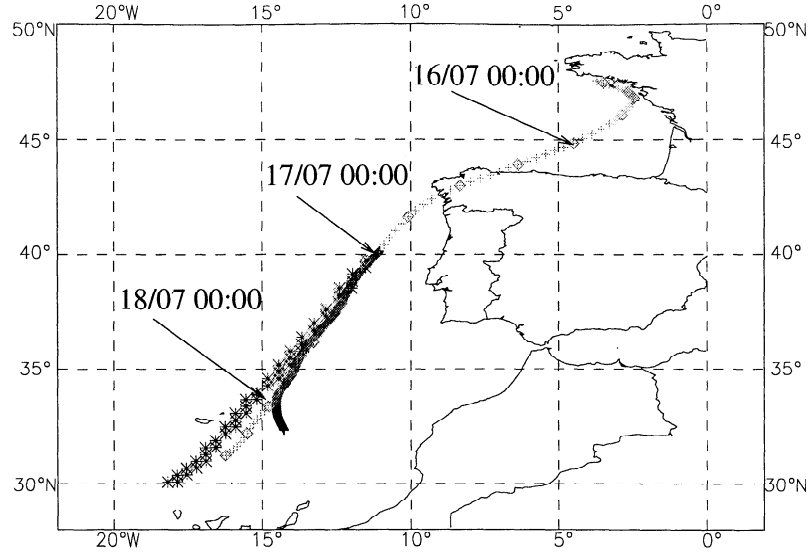

Figure 2. Observed trajectory of balloon 5 (heavy line), numerical constant altitude (500 m) trajectory passing through the release point of balloon 5 (pluses every hour, diamonds every 6 hours), and trajectory of the grid point closest to the center of mass of the passive tracer in the mesoscale simulation (stars). The grey part of the balloon trajectory corresponds to the time span 0000-2400 UTC on July, 17 1997.

July 17 is not "seen" by the model. Other cloud features that are interesting to note and that are included in the simulation are the convective activity over the Iberian Peninsula and over the Pyrenees, the frontal system that moves eastward in the upper left part of the model domain, and the recirculation in the lee of the Iberian Peninsula on July 16. This indicates that this model, with its comprehensive set of physical parameterizations and high spatial resolution, is able to simulate the different meteorological processes that control the fate of aerosol particles in the lower troposphere. Comparison with insitu observations will now be made to support this conclusion.

4.2. Comparison With the Balloon Trajectory

The evolution of the passive tracer in the model is now compared to the observed balloon trajectory. As shown in Figure 2, the center of mass of the passive tracer progresses along the balloon track with an error in position that is smaller than 1° after 24 hours of simulation, but at about a 20% higher speed. This difference is accounted to modeled wind speeds that are slightly higher than observed. We have extracted profiles from the model, following the center of mass of this tracer, in order to simulate a Lagrangian framework in the Eulerian model. Artificial advective tendencies due to errors in modeled wind speed are thus suppressed. We also chose to extract model profiles at the model grid point closest to the tracer center of mass. This leads to somewhat "noisy" time series as the extraction point jumps discontinuously every 3-5 hours from one grid point to the next. Interpolation between adjacent grid points would have led to smoother time series, but would have destroyed the internal consistency between the temperature, humidity, and cloud water profiles.

4.3. Comparison With Aircraft Data

A comparison of modeled and observed profiles of potential temperature, humidity, cloud water content, and wind speed and direction is performed. The most stringent test for a Eulerian model is the direct confrontation with in situ observations, in particular when these observations are made in a Lagrangian framework that is moving with the wind. Figures 3-7 reveal an excellent agreement between the observed and modeled profiles at the beginning of the Lagrangian experiment for all variables: boundary layer height, cloud liquid water content, wind speed and direction, thermal stratification, and water vapor mixing ratio. Note that at this time, the simulation is already running for 36 hours. Large-scale vertical transport is well represented as seen from the agreement between observed and modeled potential temperature in the free troposphere. Errors in the position of the isentropes are generally smaller than 200 m. If differential advection played a role, this has been accounted for by the model. Thus the modeled vertical velocity in the free troposphere above the MBL can be used to represent this vertical movement for the estimation of boundary layer entrainment velocities. The time evolution of the boundary layer structure, in particular that of the cloud cover, is captured. A number of fine-scale features in the observed vertical structure of the different profiles and their time evolution are also visible in the simulation, for example, the formation of a dry layer above the main inversion or the vertical stratification in wind direction and speed. The boundary layer height is, however, underestimated by about 200 m ($\approx$15%) at the end of the experiment. This is attributed to the fact that the turbulence scheme tends to distribute cloud water adiabatically in the vertical, thus modeling stratocumulus clouds, whereas dur-

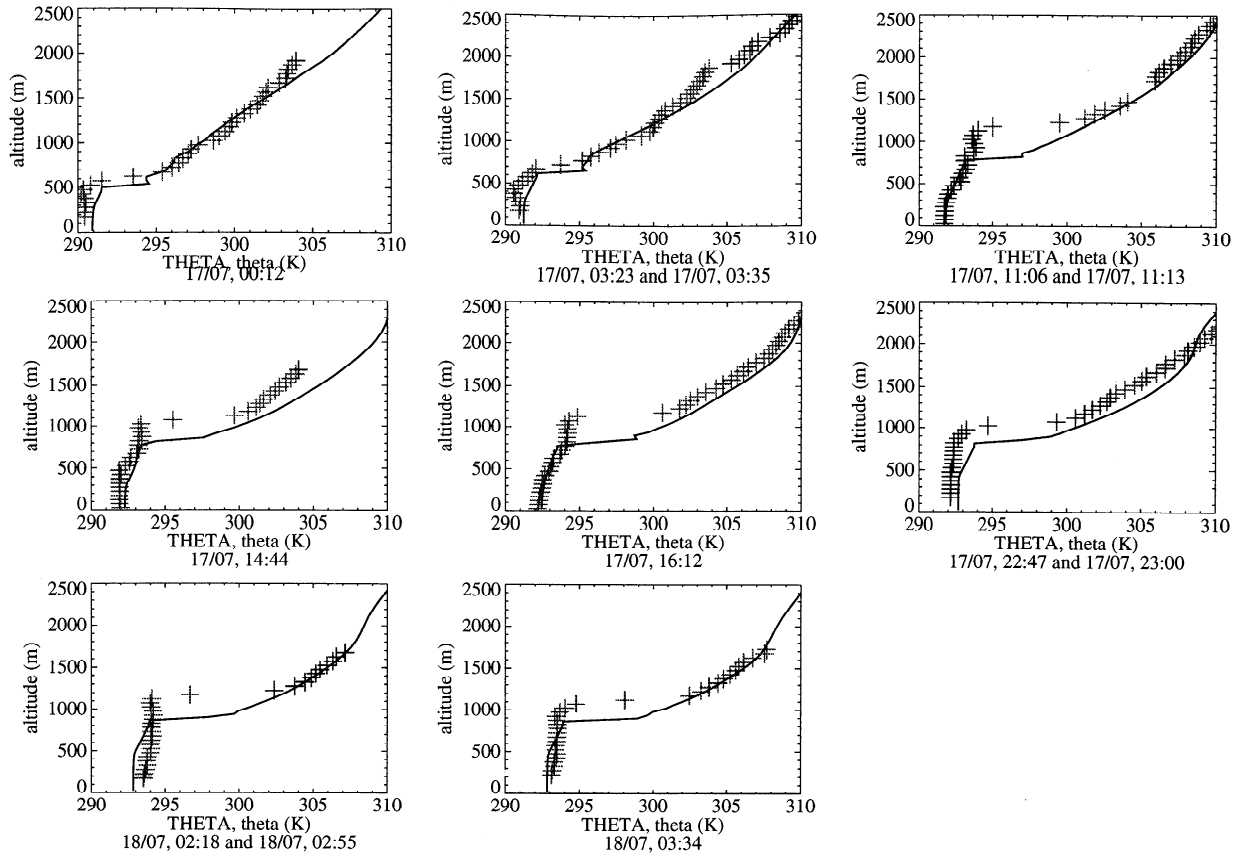

Figure 3. Vertical profiles of potential temperature as observed on selected MRF/C130 aircraft soundings (crosses) and profiles extracted from the mesoscale simulation at the corresponding time and location (solid line). The time of each sounding is indicated below each graph. In some cases, two temporal close soundings are reported on the same graph.

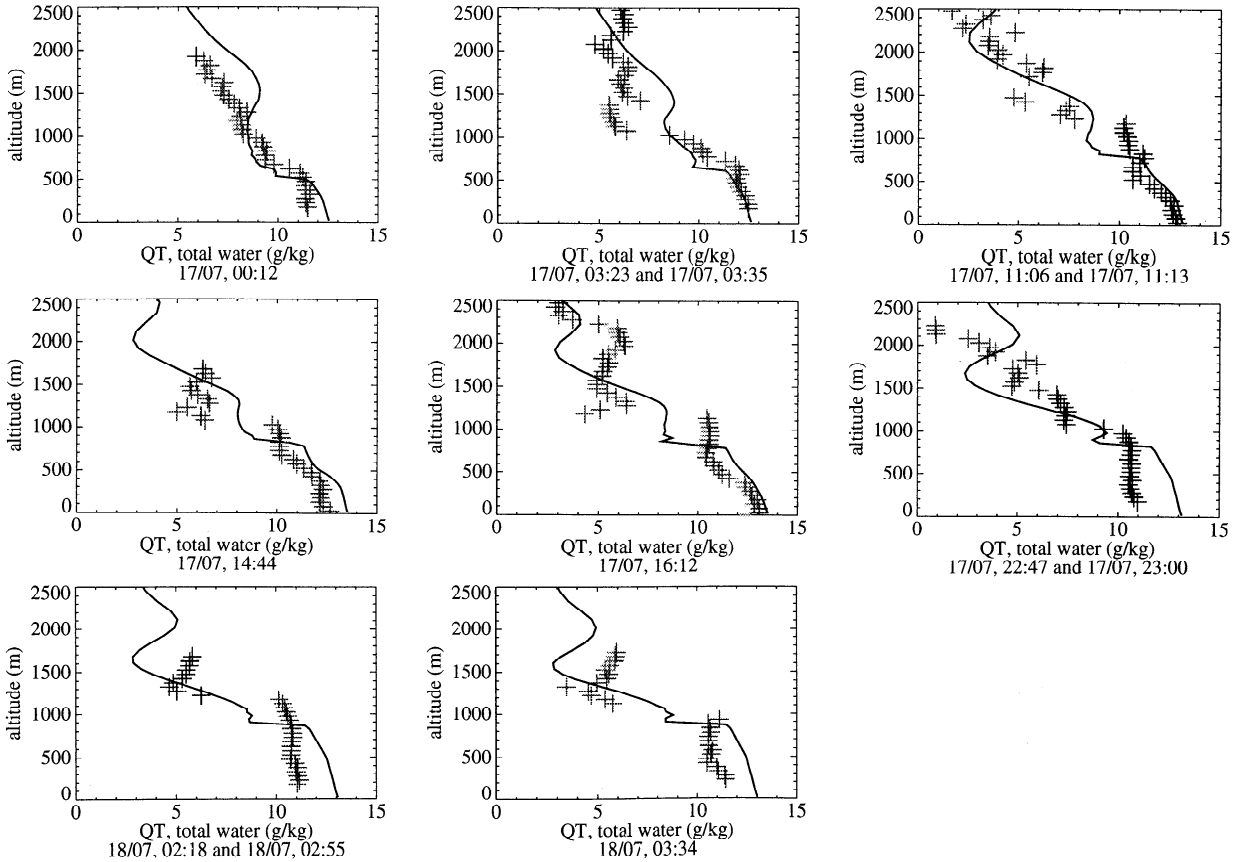

Figure 4. Same as Figure 3, but for total water mixing ratio profiles

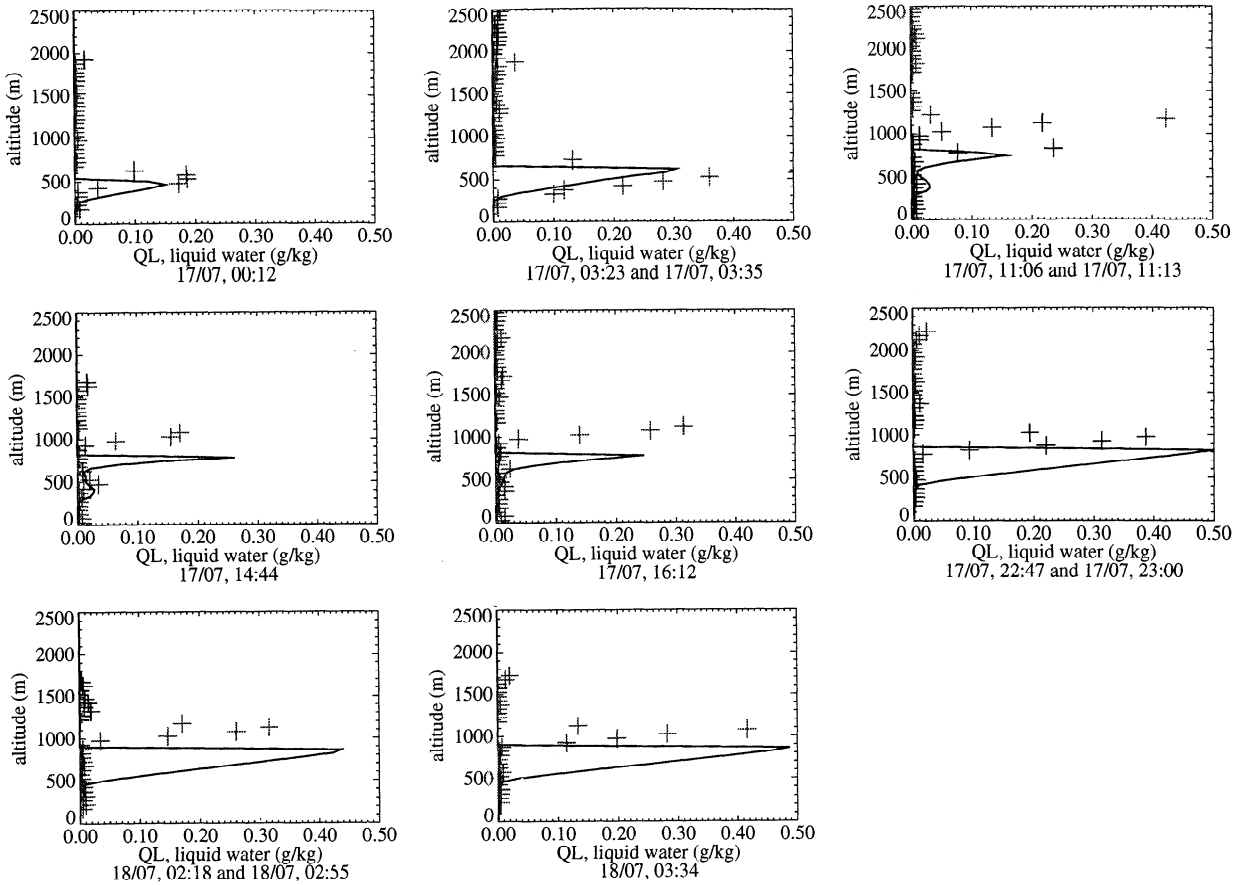

Figure 5. Same as Figure 3, but for liquid water mixing ratio profiles

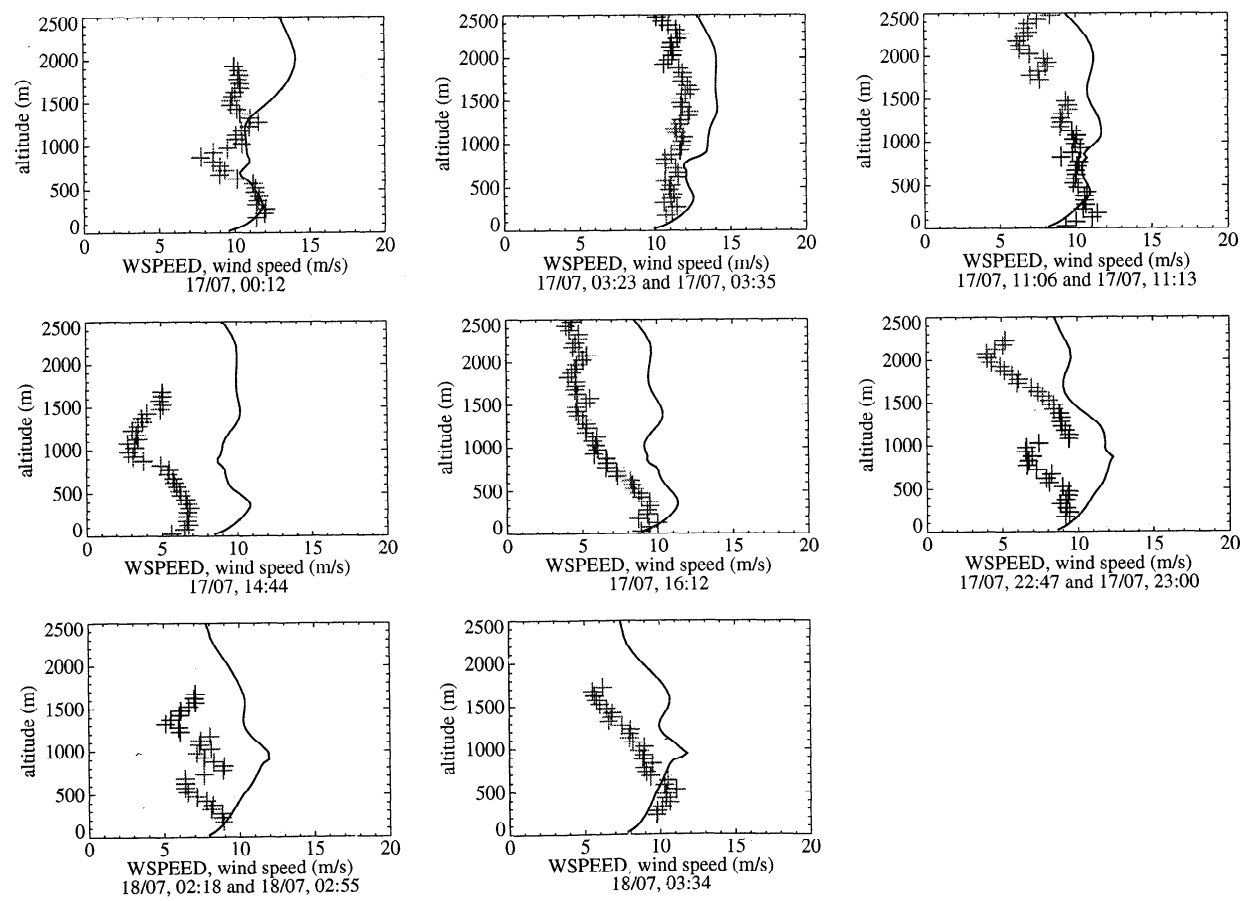

Figure 6. Same as Figure 3, but for horizontal wind speed.

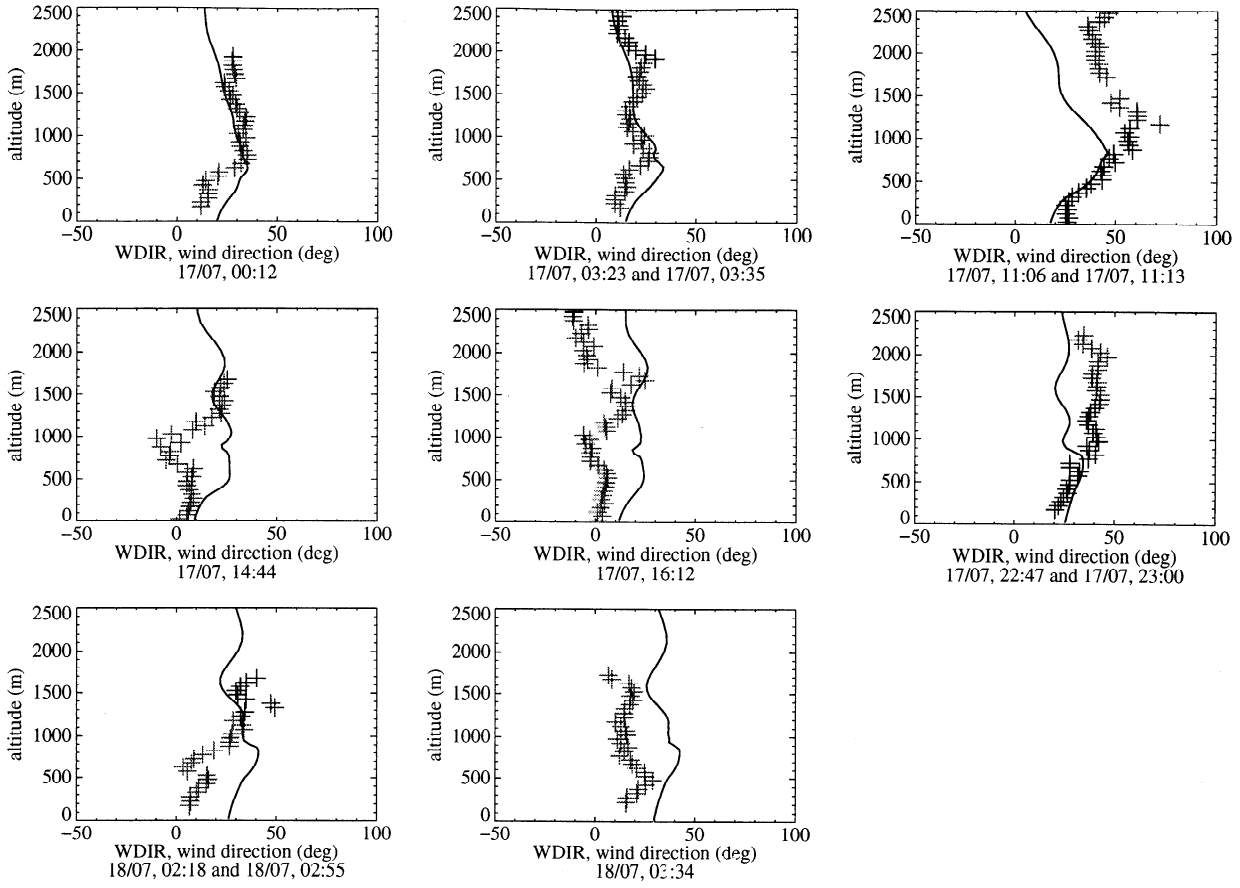

Figure 7. Same as Figure 3, but for horizontal wind direction.

ing the daytime flight on July 17 the clouds tended to be of a more convective, cumulus-type character, and occasionally penetrated a stratocumulus layer that was located under the main inversion. This problem can only be partially corrected by the fractional cloudiness scheme. A shallow convection scheme that could probably improve this shortcoming is presently under development. Modeled fractional cloud cover during noon of July 17 below the main cloud deck (not shown) can be interpreted as cumulus clouds and agrees with the visible observations reported from that flight by the mission scientist [*Osborne et al.*, 2000]. Simulated precipitation events (not shown) in the beginning and in the end of the Lagrangian experiment are also in qualitative agreement with observations.

4.4. Estimation of Entrainment Velocities

An essential parameter for aerosol and chemistry budgets in the marine boundary layer is the entrainment velocity at the inversion. It can be derived from aircraft observations [*Sollazzo et al.*, 2000], but only with a large degree of uncertainty. A complementary method is described here. As shown above, the vertical movement of the isentropes in the free troposphere is well captured by the model, which indicates that it represents the large scale vertical motion and eventual differential advection correctly. This modeled mesoscale vertical velocity together with the boundary layer growth rate may then be used to calculate the entrainment velocity. As the model underestimates the boundary layer height toward the end of the Lagrangian experiment, better results are obtained when using the observed boundary layer height. Figure 8 presents the resulting time series of the boundary layer growth velocity and the subsidence velocity at the observed inversion. The difference between both velocities yields the entrainment velocity. The modeled 28-

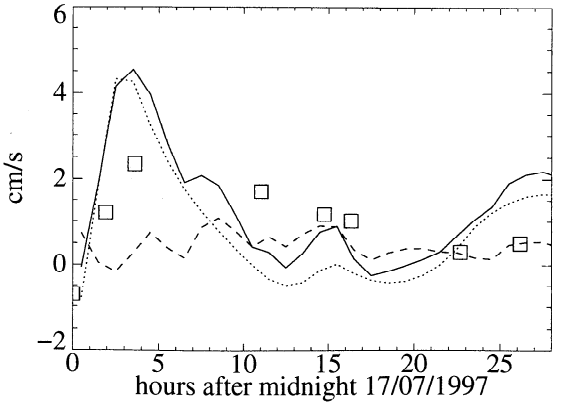

Figure 8. Modeled vertical wind speed at the boundary layer top (dashed line), observed boundary layer growth velocity (dotted line), and therefrom entrainment velocity (solid line). All curves represent hourly averaged velocities. Entrainment velocities calculated by the divergence method (adapted from *Sollazzo et al.* 2000, Figure 9) are presented for comparison (squares).

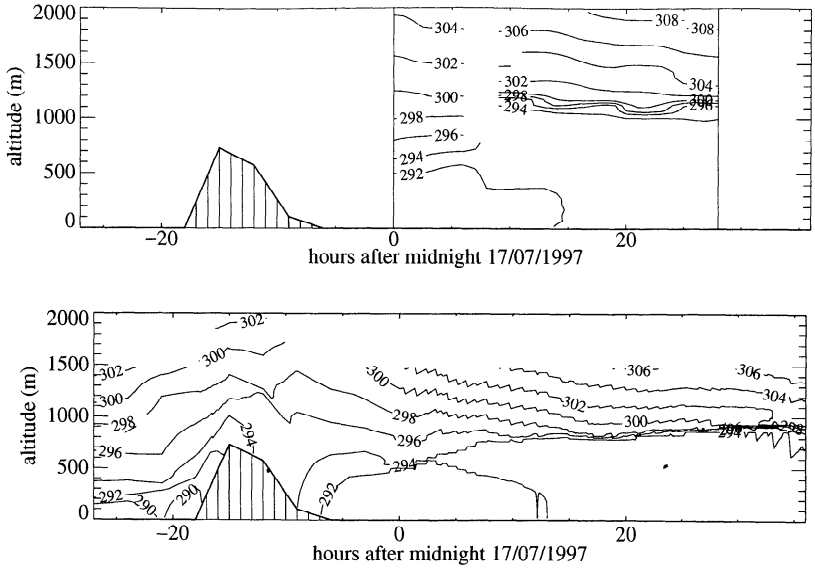

Figure 9. Time-height plot of potential temperature as (top) deduced using data from all MRF/C130 soundings and (bottom) extracted from the mesoscale simulation following the numerical trajectory up to the balloon release point and the numerical tracer thereafter. The orography of the Iberian Peninsula is presented in hatched shading. Time zero corresponds to the start of the Lagrangian experiment and the launch of the balloon.

hour averaged subsidence velocity is 0.45 cm/s, the observed average boundary layer growth velocity is 0.83 cm/s, and the resulting average entrainment velocity is 1.28 cm/s. To get a rough estimate of the precision of this value, we can use the error in the position of the isentropes (200 m) and assume an additional error of 50 m in the determination of observed MBL height. This gives an overall uncertainty of 250 m in vertical transport across the inversion for the 28 hour duration of the Lagrangian experiment; corresponding to an absolute error in vertical transport of about 0.25 cm/s, that is, 20% of the calculated average entrainment velocity.

Compared to experimentally derived entrainment velocities, the average value calculated here is equal to that derived by *Sollazzo et al.* [2000] when using the divergence method. However, maximum entrainment velocities by Sollazzo et al. are a factor of 2 smaller than what is derived here (squares in Figure 8). This may be due to a lower temporal resolution of the Sollazzo et al. time series of entrainment velocities (three data points per flight) that leads to a smoother time evolution.

4.5. History of the Boundary Layer Air Column

The history of the boundary layer air column prior to the start of the experiment is an important issue in the interpretation of Lagrangian observations of aerosols and chemical species. For this purpose, we extract the model profiles on the numerical backward trajectory to produce time-height series of potential temperature and cloud water mixing ratio for the 30 hours preceeding the launch of the balloon (Figures 9 and 10). A trajectory analysis for the air col-

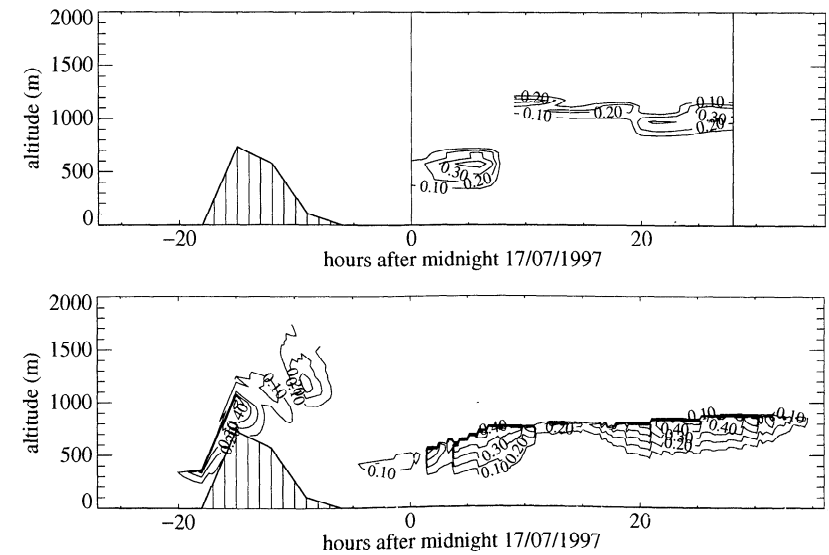

Figure 10. Same as Figure 9, but for liquid water mixing ratio. Isolines are plotted every 0.1 g/kg.

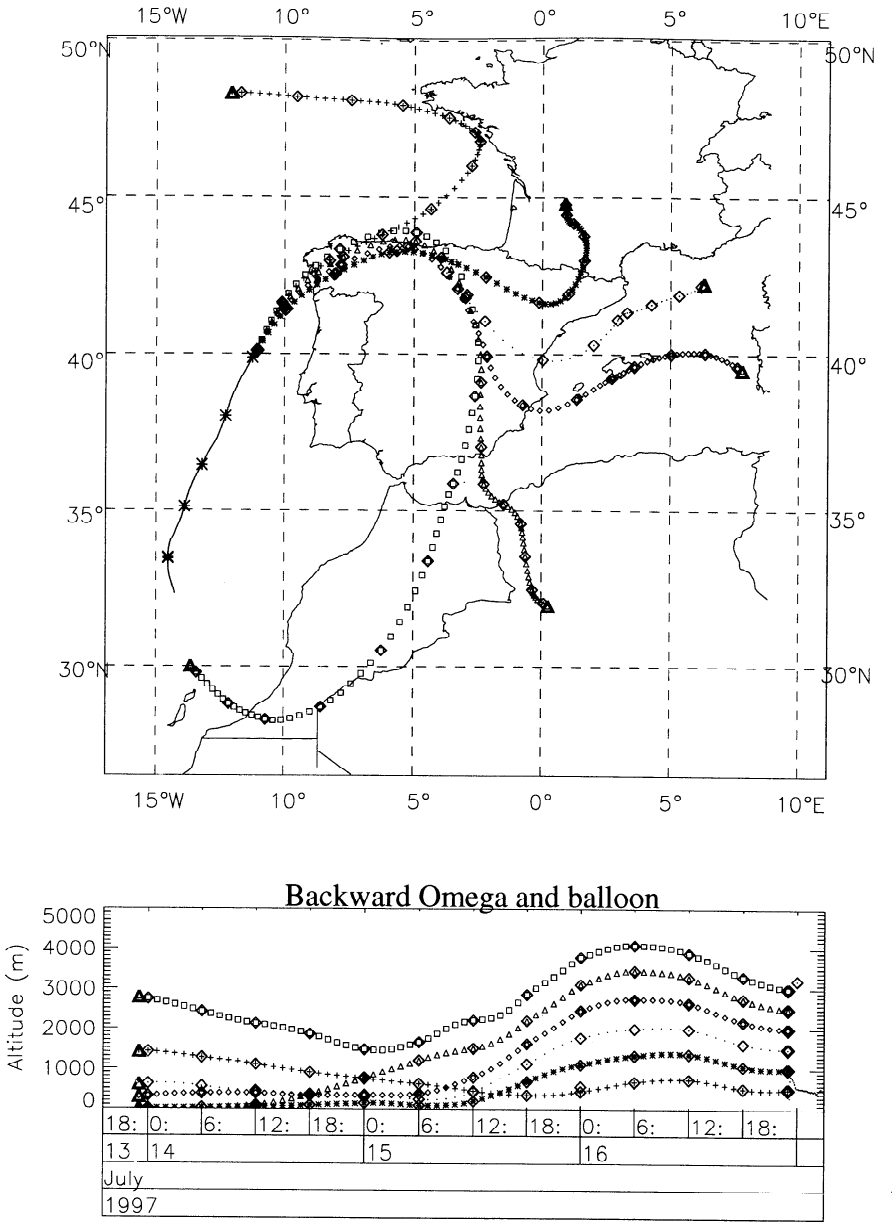

Figure 11. Trajectory analysis of the air column at the start of the Lagrangian experiment. Presented are 72-hour backward trajectories ending every 500 m above the launch point of the balloon. (top) A plan view; (bottom) diagram a side view. Diamonds are plotted every 6 hours. The thin solid line in the top view is the balloon trajectory.

umn at the starting point of the Lagrangian experiment is displayed in Figure 11. Only little differential advection occurred while the air parcel traveled over the northwestern edge of the Iberian Peninsula. Thus the concept of representing the air mass as a moving column, as required in the interpretation of Figures 9 and 10 appears to be valid.

From these figures we can deduce that the pollution layer above the MBL observed at the start of Lagrangian 2 and reaching up to 1800 m altitude was formed when the air mass traveled over the northern edge of the Iberian Peninsula. At this time, the air mass was processed by precipitating orographic clouds. The presence of these clouds is confirmed by the Meteosat 6 image in Plate 1. Presumably, most larger aerosol particles in the MBL were washed out by precipitation. It can be speculated that new particle nucleation may have taken place in the outflow of these clouds [*Clarke et al.*, 1998]. Thus, from an aerosol point of view, we can say that the boundary layer air mass was only 12-18 hours old when the Lagrangian experiment was started at midnight of July 17.

Figure 10 also shows that MBL clouds just started to form when the MRF/C130 entered the area at the start of the experiment. This explains why the formation of a bimodal aerosol spectrum was observable during the experiment [*Osborne et al.*, 2000] and why there was such a strong decrease in SO_2 concentrations from 800 ppt to 200 ppt during first

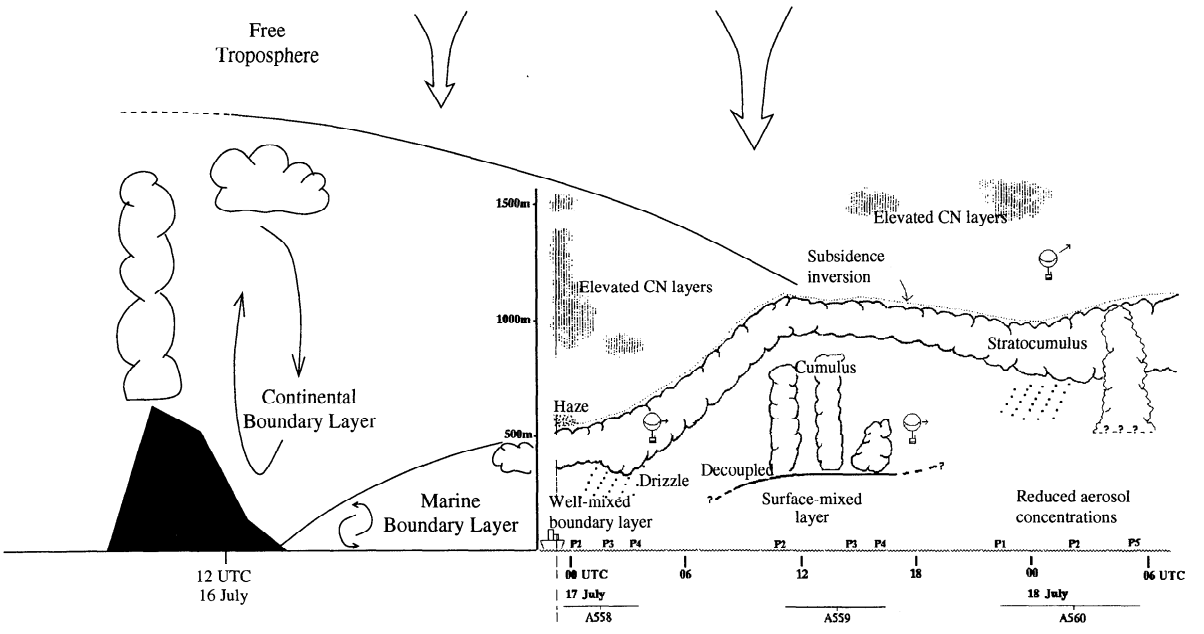

Figure 12. Schematic view of the boundary layer evolution prior to and during ACE 2 Lagrangian experiment 2. The right half of this figure (adapted from *Osborne et al.* 2000), is based on observational evidence. The left half has been reconstructed at hand of the mesoscale simulation.

the 12 hours. Had the clouds formed earlier, these processes would have been completed prior to the experiment.

From the observational analysis of the second Lagrangian experiment [*Osborne et al.*, 2000] and the mesoscale simulation presented in this paper, we have been able to put together a generalized description of a European continental outbreak of pollution over the subtropical North Atlantic. Figure 12 shows a schematic diagram of the main features of such an event. Over the continent, surface heating in the summer months together with orography-induced cloud formation produces a deep convectively driven continental boundary layer (CBL). The anthropogenic pollution produced over the continent is relatively well mixed throughout the CBL. When it is advected over the relatively cold sea, changes in surface latent and sensible heat fluxes cause a new marine boundary layer (MBL) to form, which rapidly grows as the air moves away from the coast. The CBL, having lost the strong surface forcing, collapses under the influence of the subsidence in the free troposphere which is generally present in the subtropical areas. The MBL grows within the deep pollution layer, and as the top of the MBL is generally very stable, a part of the pollution is trapped in a layer close to the surface.

Eventually, the subsidence in the free troposphere limits the growth of the MBL, and clean tropospheric air can be entrained into the MBL. It is this process which has the greatest effect on diluting the pollution in the MBL and assisting the evolution of the continental air mass into a clean maritime air mass. Washout of pollution by drizzle produced by MBL clouds is thought to be minimal as the high levels of pollution and soluble aerosol limit the size of the cloud droplets to below the size where coalescence can be effective.

Although it is not presented here, the evolution of the MBL can also modify the evolution of the aerosol characteristics. As the air moves over progressively warmer seas, the MBL deepens, moisture builds up, and stratocumulus clouds form at the top of the MBL. If the MBL gets deep enough, then the generation of turbulent kinetic energy, either by wind shear or cloud top cooling, may be not sufficient to maintain a well mixed MBL. The cloud layer then becomes decoupled from the moisture source at the surface. The MBL can then become layered with a well mixed surface layer below a cloud-containing layer. Moisture builds up in the surface mixed layer (SML), this latter becomes conditionally unstable, and cumulus clouds will grow from the top of the SML which will help maintain the stratocumulus layer by locally supplying it with moisture.

5. Conclusion

The main results of the present study can be summarized as follows:

1. An Eulerian mesoscale simulation of a typical anticyclonic situation over the North Atlantic Ocean with an associated European outbreak of air is presented. This simulation is validated against the Lagrangian observations of temperature, humidity, wind speed and direction, and cloud water content on a one-to-one basis (aircraft profiles against model profiles) over a 28 hour period. Excellent agreement is found at the start of the Lagrangian experiment which occurs after 36 hours of simulation. The overall evolution of the MBL vertical structure is captured, including some smaller-scale features such as the formation of a dry layer above the main inversion. Large-scale vertical transport in the free tropo-

sphere is also accounted for within 20% precision. Underestimation of the boundary layer height in this particular case is about 200 m (≈15%) at the end of the simulation. This should be improved by the introduction of a shallow convection scheme, presently under development. Modeled precipitation events and fractional cloudiness are in qualitative agreement with observations.

2. The model is able to reproduce most of the cloud features observed on Meteosat 6 visible imagery over the entire modeling domain, including regions close to the model boundaries, demonstrating the high quality of the ECMWF analyses.

3. A passive tracer, transported online by the model, follows the observed balloon trajectory with a position error of less than 1°. In this specific case study, the model tends to overestimate the observed wind speed, and the progression of the center of mass is about 20% faster than that of the balloon.

4. From the observed boundary layer growth and modeled vertical velocity, an average entrainment velocity of 1.28 cm/s is calculated with an estimated error of 20%. This is in close agreement with experimentally derived entrainment velocities from *Sollazzo et al.* [2000].

5. The origin of the pollution layer that overlaid the boundary layer at the beginning of the Lagrangian experiment is shown to be formed through moist orographic convection when the air mass passed over the northwestern edge of the Iberian Peninsula at 12-18 hours prior to the start of the Lagrangian experiment.

Boundary layer transport, entrainment, and cloud cycling are the key meteorological processes that control the fate of aerosol particles. Although a single case study is not sufficient to completely evaluate a model performance, the model presented here is shown to be able to simulate these processes to a good degree of precision and thus fulfills the conditions necessary for its use in future simulations. These simulations shall extend the scope of the present meteorological study through incorporation of coupled detailed aerosol and chemistry models.

Acknowledgments. This research is a contribution to the International Global Atmospheric Chemistry (IGAC) Core project of the International Geosphere-Biosphere Programme (IGBP) and is part of the IGAC Aerosol Characterization Experiments (ACE). Financial support has been allocated by CNRS (program PNCA). We thank P. Bechtold, P. Mascart, J. P. Pinty, and E. Richard for many helpfull discussions. We are grateful to R. R. Draxler for access to his trajectory model HYSPLIT_4. Analyzed meteorological fields are from the European Centre for Medium Range Weather Forecast (ECMWF). The development of the Méso-NH model is supported by CNRS/INSU.

References

Bates, T. S., B. J. Huebert, J. L. Gras, F. B. Griffiths, and P. A. Durkee, International Global Atmospheric Chemistry (IGAC) project's First Aerosol Characterization Experiment (ACE 1): Overview, *J. Geophys. Res., 103*, 16,297–16,318, 1998.

Bechtold, P., C. Fravalo, and J. P. Pinty, A model of marine boundary layer cloudiness for mesoscale applications, *J. Atmos. Sci., 49*, 1723–1744, 1992.

Bougeault, P., and P. Lacarrère, Parameterization of orography-induced turbulence in a meso-beta model, *Mon. Weather Rev., 117*, 1872–1890, 1989.

Bretherton C. S., and R. Pincus, Cloudiness and marine boundary layer dynamics in the ASTEX Lagrangian experiments, 1, Synoptic setting and vertical structure, *J. Atmos. Sci., 52*, 2707–2723, 1995.

Businger, S., S. R. Chiswell, W. C. Ulmer, and R. Johnson, Balloons as a Lagrangian measurement platform for atmospheric research, *J. Geophys. Res., 101*, 4363–4376, 1996.

Businger, S., R. Johnson, J. Katzfey, S. Siems, and Q. Wang, Smart tetroons for Lagrangian air mass tracking during ACE 1, *J. Geophys. Res., 104*, 11709–11722, 1999.

Clarke, A., J.L. Varner, F. Eisele, R.L. Mauldin, D. Tanner, and M. Litchy, Particle production in the remote marine atmosphere: Cloud outflow and subsidence during ACE 1, *J. Geophys. Res., 103*, 16,397–16,409, 1998.

Dore, A.J., D.W. Johnson, S.R. Osborne, T.W. Choularton, K.N. Bower, M.O. Andreae, and B.J. Bandy, Evolution of boundary layer aerosol particles due to in-cloud chemical reactions during the second Lagrangian experiment of ACE-2, *Tellus B*, in press, 2000.

Draxler, R. R., and G. D. Hess, An overview of the HYSPLIT_4 modeling system for trajectories, dispersion and deposition, *Aust. Meteorol. Mag., 47*, 295–308, 1998.

Huebert, B. J., A. A. Pszenny, and B. Blomquist, The ASTEX/MAGE Experiment, *J. Geophys. Res., 101*, 4319–4329, 1996.

Johnson, D. W. et al., An overview of the Lagrangian experiments undertaken during the North Atlantic Regional Aerosol Characterization Experiment (ACE-2), *Tellus, Ser. B*, in press, 2000.

Kain, J. S., and J. M. Fritsch, A one-dimensional entraining/ detraining plume model and its application in convective parameterizations, *J. Atmos. Sci., 47*, 2784-2802, 1990.

Kessler, E., On the distribution and continuity of water substance in atmospheric circulations, *Meteorol. Monogr., 10* (32), 84 pp., 1969.

Lafore, J. P., et al., The Meso-NH Atmospheric Simulation System, I, Adiabatic formulation and control simulations, *Ann. Geophys., 16*, 90-109, 1998.

Mari, C., K. Suhre, T. S. Bates, J. E. Johnson, R. Rosset, A. R. Bandy, F. L. Eisele, R. L. Mauldin III, and D. C. Thornton, Physico-chemical modeling of ACE 1 Lagrangian B, 2, DMS emission, transport, and oxidation at the mesoscale, *J. Geophys. Res., 103*, 16,457–16,473, 1998.

Mari, C., K. Suhre, R. Rosset, T. S. Bates, B.J. Huebert, A. R. Bandy, D. C. Thornton, and S. Businger, One-dimensional modeling of sulfur species during the Fisrt Aerosol Characterization Experiment (ACE 1) Lagrangian B, *J. Geophys. Res., 104*, 21,733–21,749, 1999.

Morcrette, J.-J., Impact of changes of the radiation transfer parameterizations plus cloud optical properties in the ECMWF model, *Mon. Weather Rev., 118*, 847–873, 1989.

Nickerson, E. C., E. Richard, R. Rosset, and D. R. Smith, The numerical simulation of clouds, rain, and airflow over the Vosges and Black Forest mountains: A meso-β model with parameterized microphysics, *Mon. Weather Rev., 114*, 398–414, 1986.

Osborne, S. R., et al., Evolution of the aerosol, cloud and boundary layer dynamic and thermodynamic characteristics during the second Lagrangian experiment of ACE-2, *Tellus, Ser. B*, in press, 2000.

Raes, F., et al., ACE-2 overview paper, *Tellus, Ser.B*, in press, 2000.

Redelsperger, J. L., and G. Sommeria, Méthode de représentation de la turbulence d'échelle inférieure à la maille pour un modèle tri-dimensionnel de convection nuageuse, *Boundary Layer Meteorol., 21*, 509–530, 1981.

Russel, L. M., D. H. Lenshow, K. K. Laursen, P. B. Krummel, S. T. Siems, A. R. Bandy, D. C. Thornton, and T. S. Bates, Bidirectional mixing in an ACE 1 marine boundary layer over-lain by

a second turbulent layer, *J. Geophys. Res., 103*, 16,411-16,432, 1998.

Sollazzo, M.J., L.M. Russell, D. Percival, S. Osborne, R. Wood, and D.W. Johnson, Entrainment rates during ACE 2 Lagrangian experiments calculated from aircraft measurements, *Tellus, Ser.B*, in press, 2000.

Suhre, K., and R. Rosset, DMS oxidation and turbulent transport in the marine boundary layer: A numerical study, *J. Atmos. Chem., 18*, 379–395, 1994

Suhre, K., et al., Physico-chemical modeling of ACE 1 Lagrangian B. 1. a moving column approach. *J. Geophys. Res., 103*, 16433–16456, 1998.

Wang, Q., D. H. Lenschow, L. Pan, R. D. Schillawski, G. L. Kok, K. Laursen, L. M. Russell, A. Bandy, D. Thornton, and K. Suhre, Characteristics of the marine boundary layers during two Lagrangian measurements, 2, Turbulence structure, *J. Geophys. Res., , 104*, 21,767–21,784, 1999.

T.S. Bates, Pacific Marine Environmental Laboratory, NOAA, Seattle, WA 98115.

D.W. Johnson, S. Osborne, and R. Wood, Meteorological Research Flight, Meteorological Office, Farnborough, GU146TD, England, U.K.

C. Mari, R. Rosset, and K. Suhre, Laboratoire d'Aérologie, UMR CNRS/Université Paul Sabatier, 31400 Toulouse, France. (e-mail: marcaero.obs-mip.fr)

F. Raes, European Commission, Joint Research Centre, VA-21020, Ispra, Italy.

(Received October 25, 1999; revised February 24, 2000; accepted February 28, 2000.)